Gravitational Recoil and Astrophysical Impact

Ulrich Sperhake

Abstract Asymmetric emission of gravitational waves from astrophysical sources leads to a net flux of linear momentum from the source and, by momentum conservation, imparts a gravitational recoil on the emitting source. Numerical relativity simulations have revealed that this effect can lead to astonishingly large kick velocities, so-called *superkicks*, of several thousand km/s in the inspiral and merger of black-hole binaries. We here discuss the calculation of the recoil in black-hole spacetimes and the astrophysical repercussions of such large kicks, in particular related to the possible displacement or ejection of supermassive black holes from their host galaxies. We also discuss possible mechanisms that would make superkicks improbably to occur in astrophysical binaries and thus explain why most, if not all, galaxies observed in this regard appear to harbor a black hole at their center.

1 Introduction and motivation

A dictionary definition of the term *recoil* is given as the act of "moving abruptly backward as a reaction on firing a bullet, shell, or other missile"; see e.g. [1]. It may appear at first glace surprising that this effect plays an important role for astrophysical black holes (BHs). After all, BHs are (at classical level) black objects and not supposed to emit anything, not even light. And yet, the gravitational recoil or "kick" of BHs is generally regarded an important dynamical feature in a variety of astrophysical scenarios involving, in particular, supermassive BHs (SMBHs). The role of the "missile" mentioned in the above definition in this case is played by the

Ulrich Sperhake
Department of Applied Mathematics and Theoretical Physics, University of Cambridge, Wilberforce Road, Cambridge CB3 0WA, United Kingdom
California Institute of Technology, 1200 E California Boulevard, Pasadena, CA 91125, USA
Department of Physics and Astronomy, The University of Mississippi, University, MS 38677, USA
e-mail: U.Sperhake@damtp.cam.ac.uk

gravitational waves (GWs) generated in the inspiral and merger of BH binaries. In addition to energy, GWs also carry away linear momentum from their source and if the emission of linear momentum is anisotropic, the net loss of momentum is compensated for by a recoil of the emitting source. We note in this context that kicks also arise in supernova core collapse, mostly through anisotropic emission of neutrinos; see e.g. [2]. While these are also of high relevance in astrophysics, our focus here will be on gravitational recoil of black holes generated through GW emission.

The fact that anisotropic gravitational radiation will impart a kick on the emitting source was already realized in the early 1960s [3, 4]; see also [5]. The determination of accurate prediction for the magnitude of the resulting kick velocities, however, represents a major challenge given the high complexity of the dynamical processes responsible for the GW generation. It is only through the use of complex numerical codes, that a quantitative exploration of BH kicks has become possible in the last ~ 10 years. As we shall discuss in more detail below in Sec. 2, kick velocities range over several orders of magnitude depending on the binary constituents' parameters. For interpreting these numbers, we need some reference of astrophysically relevant kick velocities. Such reference numbers are given by the escape velocities from the astrophysical object hosting the BHs. These escape velocities vary with the mass of the host and typical values are $v_{\rm esc} \approx 30$ km/s for globular clusters, $20-100$ km/s for dwarf galaxies and $\sim 1\,000$ km/s for giant elliptic galaxies; cf. Fig. 2 in [6]. Recoils in the range of these numbers would then be able to displace or even eject the merger remnant BH from the centre of its host with wide ranging astrophysical implications.

Observations of galaxies provide strong evidence that most if not all galaxies harbor massive dark objects which are most plausibly interpreted as BHs [7, 8]. Observations furthermore demonstrate that the properties of the BHs are correlated with properties of the host galaxies such as their luminosity, mass and velocity dispersion [7, 8, 9, 10]. The formation of SMBHs by redshift $z \approx 6$, as suggested by the presence of quasars at such rather early times in the universe, is often described in terms of hierarchical or "bottom-up" growth through accretion and BH mergers; see for example [11]. At high redshift $z \geq 10$, the dark matter halos hosting the BHs have escape velocities of less than about 150 km/s, so that even moderate kicks would be sufficient to eject BHs [12]. Efficient ejection of BHs does not only have consequences for the merger rate of BHs [13, 14] but also leads to BH depleted globular clusters [15] and may necessitate accretion above the Eddington limit to ensure a sufficiently rapid assembly of SMBHs [16].

BHs ejected or displaced from their hosts centers may also be directly observable in electromagnetic radiation. Several candidates have indeed been identified, although the interpretation of the data is not unambiguous in these cases. Komossa *et al* [17], for example, have observed a blue shift corresponding to 2650 km/s of the broad-line region relative to the narrow-line region in the quasar J0927+2943. As we shall see in Sec. 2 below, this magnitude is about half of the maximum recoil velocities generated in BH inspiral and merger and, thus, may represent a BH kicked out of its host. Alternatively, however, the observed features could be explained in terms of a superposition of two active galactic nuclei (AGN) or a binary

BH system [18, 19]. Similarly, the galaxy CID−42 shows features compatible with an inspiraling AGN pair and an AGN with kick velocity $\sim 1\,300$ km/s. Using hydrodynamic galaxy merger simulations coupled to radiative transfer, Blecha *et al* [20] find both, a double-AGN and a recoil model compatible with the observations and a clear identification of the system is not possible with the present data. A similar example is given by the galaxy merger remnant COSMOS J100043+020637 which contains two optical nuclei about 2 kpc apart [21]. These can be interpreted as a BH ejected or displaced from the galactic centre. Further electromagnetic signatures of BH kicks include tidal disruptions of stars by the moving BH and resulting X ray flares [22, 23, 24] and repeated flares caused by a displaced BH oscillating on a scale comparable to the accretion torus [25]. Also, the relative motion between a recoiling BH and the accreting material would introduce vibrations in the density of the shock cone with frequencies similar to those observed in quasi-periodic oscillations of X ray sources [26]. For a more comprehensive discussion of the electromagnetic signatures resulting from recoiling BHs, the reader is referred to Komossa's review [27].

A clear understanding of the kick magnitudes and its dependency on the BH binary parameters is clearly necessary for the interpretation of the observations as well as theoretical modeling of galaxies, structure formation in the universe and the assembly of SMBHs. In the next section we discuss the progress made in this direction focusing on numerical relativity applications.

2 Calculation of the recoil

By simple symmetry considerations the inspiral and merger of a binary system composed of identical compact objects cannot generate a net recoil. Consider for example two non-spinning BHs of equal mass and let us denote the kick velocity resulting from their coalescence by $\mathbf{v}_{\rm kick}$. Because the two BHs are identical, the configuration obtained by reflection of the system across the center of mass, will be identical to the original one but invert the recoil velocity so that $\mathbf{v}_{\rm kick} = -\mathbf{v}_{\rm kick}$ which is only satisfied by $v_{\rm kick} = 0$. In order to obtain a non-vanishing recoil, we therefore need to break the symmetry of the system under consideration. In the case of BH binaries in vacuum, this can be achieved either by considering BHs of unequal masses or rotating BHs with different spins.

The recoil of unequal-mass but non-spinning BH binary systems was first studied systematically by Fitchett [28] who used a quasi-Newtonian approach modeling the binary as two point masses in Keplerian orbit. For binaries with zero eccentricity, Fitchett's calculation suggests a functional dependency $v_{\rm kick} \sim \eta^4\sqrt{1-4\eta}$ of the kick velocity on the mass ratio which we here define in terms of the individual BH masses m_1 and m_2 through

$$q \equiv \frac{m_2}{m_1} \leq 1\,, \qquad \eta \equiv \frac{m_1 m_2}{(m_1+m_2)^2} = \frac{q}{(1+q)^2}\,. \tag{1}$$

Note that there is no general convention in the literature but here we label the BHs such that $m_2 \leq m_1$. η is often referred to as the "dimensionless mass-ratio parameter". Fitchett's calculation also includes a generalization to eccentric orbits, but due to the circularizing effect of GW emission [29] the eccentricity of BH binaries is expected to vanish with high precision in the late inspiral stage which dominates the net emission of linear momentum.

The main question left open by these calculation is the actual magnitude of the kick or, in other words, the proportionality constant in the functional relation between the kick and mass ratio. The determination of these numbers only became possible with the breakthroughs of numerical relativity [30, 31, 32] which opened up the regime of dynamic, strong-field interaction of BH binaries for precision studies. The recoil generated in the merger of non-spinning, unequal-mass binaries was indeed one of the first applications of numerical relativity [34, 35, 36] after the breakthroughs. The most extended study of the η parameter space was performed by Gonzáles *et al.* [35] who simulated a large number of binaries with mass ratios ranging from $q = 1$ to $q = 1/4$. Based on Fitchett's calculations, they fit their data using the relation

$$v_{\rm kick} = A\eta^2\sqrt{1-4\eta}\,(1+B\eta)\,, \tag{2}$$

and determine the parameters $A = 1.2\times 10^4$ km/s, $B = -0.93$. The numerical results of their study, augmented by data for $q = 1/10$ [33], are displayed in Fig. 1 together with the fit (2) as well as an alternative fit by [34] and an effective-one-body prediction by [37]. The maximum kick of non-spinning BH binaries determined from these simulations is 175.2 ± 11 km/s realized for $\eta = 0.195 \pm 0.005$. This value is

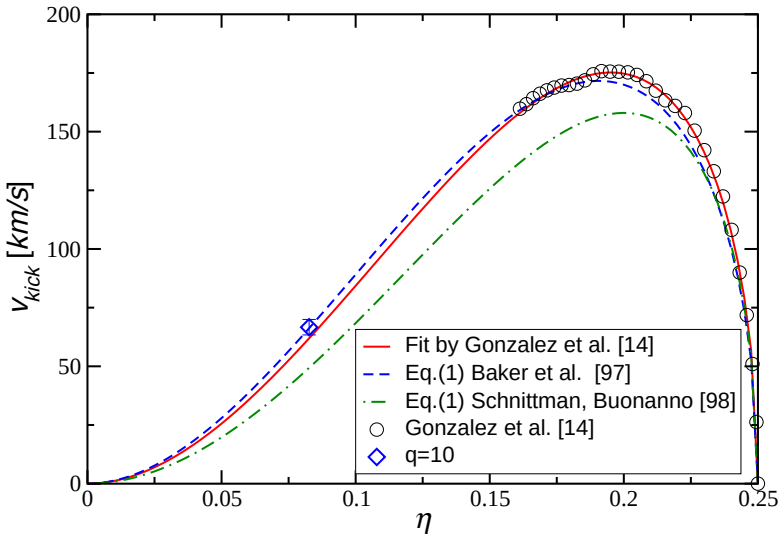

Fig. 1 Recoil velocity resulting from the merger of non-spinning BH binaries with dimensionless mass-ratio parameter η. The circle and diamond symbols represent numerical relativity results and the curves various fits or predictions. Figure taken from [33].

large enough to eject BHs from globular clusters or dwarf galaxies but well below the escape velocity from giant galaxies.

The inclusion of BH spins significantly complicates the calculation of the recoil. In addition to the mass ratio, there are now 6 spin parameters, 3 for each BH. A first exploration of the spins' impact on the emission of linear momentum through GWs was made by Kidder [38] using post-Newtonian (PN) calculations. The resulting linear momentum is composed of a contribution due to the unequal masses, the Fitchett contribution, and a term due to the spin-orbit coupling. Again, the determination of precise numbers became possible through numerical relativity calculations. These first considered spins parallel to the orbital angular momentum $\boldsymbol{L}$, i.e. spins aligned or anti-aligned with $\boldsymbol{L}$. As discussed above, a non-zero kick is only realized in these cases when the BHs have different masses or different spins. A variety of configurations were analysed in Refs. [39, 40, 41] and predict kicks of up to 500 km/s. This maximum is obtained by extrapolating from the simulations to the maximal spin magnitude $\chi \equiv a/m = 1$, where a is the Kerr spin parameter and m the BH mass. Kidder's work, however, suggests a separate contribution to the total kick pointing out of the orbital plane. Based on this motivation, González *et al.* [42] and Campanelli *et al.* [43, 44] simulated equal-mass BH binaries with spins oriented perpendicular to $\boldsymbol{L}$, i.e. in the orbital plane, but opposite to each other. The astonishing result of these simulations were kick velocities of a few thousand km/s with an extrapolated (to $\chi = 1$) of 4000 km/s, often referred to as *superkicks*. Figure 2 illustrates the BH trajectories in an inspiral lasting ~ 2 orbits; during inspiral, the orbital plane moves up and down along the direction of the orbital angular momentum (pointing upwards in the figure) and, after merger, the single BH moves in that direction with $v_{\rm kick}$. Closer investigation of these superkicks revealed that $v_{\rm kick}$ has a sinusoidal dependence on the angle between the spin of either hole and the line-of-sight between the holes at the start of the simulation which corresponds to a dependency on the orbital phase; cf. Fig. 4 in [45]. An intuitive interpretation of

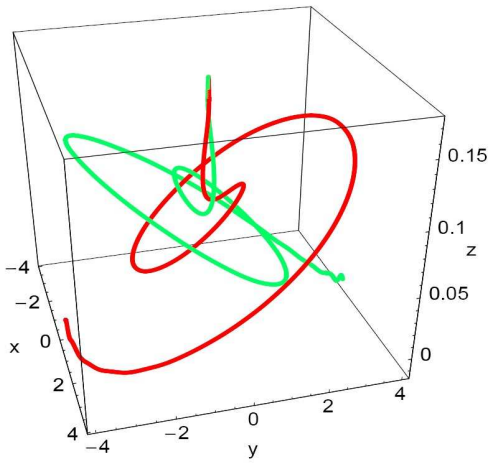

Fig. 2 Trajectories of the BHs in a superkick configuration with individual spins oriented in the orbital plane but opposite to one another.

the superkick phenomenon is provided in Fig. 5 of [46]. The motion of the orbital plane up and down along the direction of $\boldsymbol{L}$ is a consequence of the frame dragging exerted on each binary member by the other hole. This motion introduces a Doppler shift to the emitted gravitational radiation and, thus, an asymmetry in the amount of GWs emitted in the corresponding directions. The net effect is an asymmetry in the $l = 2$, $m = \pm 2$ GW multipoles [45] and a net amount of linear momentum emitted in GWs whose magnitude depends on the precise phase in this cyclic process where the merger puts an end to this process.

A further increase in the maximum kick in BH binary inspiral has been realized by Lousto & Zlochower [47, 48] by combining the superkick with the "orbital hang up" effect. The orbital hang up arises in the inspiral of BHs with spins aligned with the orbital angular momentum and results in a larger number of orbits at small separation shortly before merger and, consequently, increased emission of GW energy by about a factor of two compared with the non-spinning counterpart [49, 50]. For equal masses and spins, these configurations do not result in a net linear momentum due to the symmetry argument mentioned abode. For BH spins *partially* aligned with $\boldsymbol{L}$ such that the spin projections onto the orbital plane are equal in magnitude and opposite in direction, however, Lousto & Zlochower were able to optimize the increased GW emission of the hang-up effect with the net-emission of linear momentum and observed even larger kicks of up to $5\,000$ km/s realized for inclination angles of about 45° and extrapolated to maximal spins $\chi = 1$.

A main goal for the modeling of gravitational recoil in BH binaries is the generation of a "black box" or fitting formula that takes as input the parameters of the binary and returns the kick velocity as output. We have already seen such a formula for the simple case of non-spinning binaries in Eq. (2). Various suggestions of varying degrees of complexity have been made to generalize such a formula for spinning binaries. Campanelli *et al.* [43], have proposed the following expression for modeling superkicks, but not including the hang-up kicks. Here we again denote the dimensionless spin parameters by χ with index 1 or 2 for either hole. Boldface characters represent vectorial quantities and we use sub or super scripts $\perp$ and $||$ to denote vector components perpendicular and parallel to the orbital angular momentum $\boldsymbol{L}$, respectively. With this notation we have[1]

[1] We use here the notation of Ref. [51] which differs from that of [43] by the convention that $q \equiv m_2/m_1 \leq 1$.

$$\boldsymbol{v}_{\rm kick}(q,\boldsymbol{\chi}_i) = v_m \boldsymbol{e}_1 + v_\perp (\cos\xi\, \boldsymbol{e}_1 + \sin\xi\, \boldsymbol{e}_2) + v_{||} \boldsymbol{e}_{||}\,,$$

$$v_m = A\eta^2 \frac{1-q}{1+q^5}\,(1+B\eta)\,,$$

$$v_\perp = H\frac{\eta^2}{1+q}\left(q\boldsymbol{\chi}_2^{||} - \boldsymbol{\chi}_1^{||}\right),$$

$$v_{||} = K\frac{\eta^2}{1+q}\cos(\Theta-\Theta_0)\left|q\boldsymbol{\chi}_2^{\perp} - \boldsymbol{\chi}_1^{\perp}\right|. \qquad (3)$$

Here $(\boldsymbol{e}_1, \boldsymbol{e}_2, \boldsymbol{e}_{||})$ is an orthonormal basis with $\boldsymbol{e}_{||}$ pointing along $\boldsymbol{L}$, ξ is angle found to be $\sim 145^\circ$ for a wide variety of quasi-circular configurations [52] and Θ is the angle between $q\boldsymbol{\chi}_2 - \boldsymbol{\chi}_1$ and the line of sight between the BHs at the time of "merger". This angle is determined by the phase angle mentioned above and enters the superkick in the sinusoidal form discussed in this context. For most astrophysical applications, this angle is only known in the form of a statistical distribution, commonly chosen to be flat in $[0, 180^\circ$. The kick magnitude is then determined by the fitting coefficients which are $A = 1.2\times10^4$ km/s, $B = -0.93$ [35], $H = (6.9\pm0.5)\times10^3$ km/s [53], $K = (6.0\pm0.1)\times10^4$ km/s [44].

Various attempts have been made to extend Eq. (3). A systematic spin expansion of the recoil has been explored by Boyle *et al.* [54, 55] exploiting all possible symmetry conditions. The resulting expansion is yet to be calibrated by numerical relativity simulations, however. An extension of Eq. (3) that includes the hang-up kick is given in Ref. [48] and further elaboration through inclusion of various higher-order terms has resulted in a further ~ 10 % increase in the maximal kick, an effect dubbed *cross kick* [56]. A detailed discussion of these formulae is beyond the scope of this work and we refer the interested reader to the references for further information.

3 Open questions

The accurate determination of kick velocities generated through GW emission in the merger of BH binaries has made tremendous progress over the last decade and the discovery of the superkicks remains one of the most astonishing results obtained with numerical relativity simulations to date. Still, a good deal of work needs to be done before the kick phenomenon can be regarded as comprehensively understood. In this section we will list our pick of the most important questions that need to be resolved in future work.

1) A complete kick formula: We have seen that asymmetries in the BH spins introduces significantly larger recoil velocities than unequal mass parameters do for non-spinning BHs. The inclusion of spins and the associated 6 parameters is therefore

absolutely necessary for obtaining astrophysically helpful kick formulas and, as we have seen, plenty of work has already been invested in this direction. Nevertheless, a full exploration of the parameter space will require more numerical simulations. The majority of simulations used to calibrate existing formulae for spinning binaries have been performed for equal-mass systems. While there have been explorations of spinning-unequal mass BHs [57, 43, 58, 52], the dependence of the superkick and hang-up kicks, in particular, is not yet known with sufficient precision. The good news is that this question can be addressed by simply performing more numerical simulations. Even though this requires considerable resources given the high dimensionality of the parameter space, it appears straightforward to fill in the missing gaps in the kick formulae.

2) Parameter evolution during the inspiral: A conceptually more delicate problem arises from the BH parameters that are actually used as input for existing (or future) kick formulae. Numerical simulations typically start a few orbits prior to merger of the binary. For a given system this provides accurate estimates for the recoil magnitude because the emission of linear momentum is entirely dominated by the last few orbits prior to merger; see e.g. Fig. 9 in [45]. Astrophysical studies involving BHs, however, typically make predictions (typically in statistical form for an ensemble of BHs) for the parameters at a time when the BHs are still much farther apart; see e.g. [59]. The ensuing inspiral from such large scales to the late inspiral regime of numerical relativity covers hundred of thousands of orbits if not more. The question then is how this long inspiral phase will modify the BH parameters and how we can generate legitimate input for kick formulae valid for the last few orbits. This question is largely of statistical nature and in practice we will not be concerned too much with how the parameters of one particular binary are affected, but rather how the inspiral gradually influences and distorts a parameter distribution. This question has first been explored by Bogdanović *et al.* [60] who use PN calculations [61] to evolve an ensemble of BHs with mass ratio $q = 9/11$, maximal spin magnitudes and isotropic distribution of the spin directions from a separation $d = 1\,000\,M$ to $d = 10\,M$ where M is the total BH binary mass. They find this ensemble to remain isotropic, i.e. statistically unchanged during the inspiral. As we shall see in the next section this does not remain the case when we start with initially anisotropic ensembles. For application of kick formulae, this necessitates a prescription for how the statistical properties of a given distribution changes under the inspiral.

3) Astrophysical observations of SMBHs in galaxies: The third question is of astrophysical nature. As mentioned above, astrophysical observations suggest that large galaxies ubiquitously harbor SMBHs. On the other hand, the magnitude of superkicks or hangup kicks comfortably exceeds the escape velocity from even the most massive galaxies and thus would suffice to eject BHs from their hosts. Why then do we not observe more galaxies without a BH? Possibly, we simply need a larger statistical sample of observations. Schnittman & Buonanno [37] have estimated the statistical distribution of kicks generated in BH mergers using effective-one-body calculations for an ensemble of BH binaries with $q \in [0.1, 1]$, $\chi_i = 0.9$

and find that about 12 % of the mergers result in $v_{\rm kick} > 500$ km/s and about 3 % in $v_{\rm kick} > 1000$ km/s. Recent work by Gerosa & Sesana [62] models the consequences of superkicks in the merger history of brightest-cluster galaxies and find that the BH occupation fraction f of these galaxies is $0.9 < f < 0.99$ in the local universe. A statistically robust determination of the frequency of BH ejection therefore seems to require hundreds of observations which will be made possible by future thirty-meter-class telescopes. An alternative explanation of ubiquitous presence on SMBHs in galaxies may be that superkicks, while theoretically possible, are statistically suppressed by some mechanism. This could be achieved, for example, by the alignment of BH spins with the orbital angular momentum through torques from accreting gas in gas-rich mergers [60]. The degree of alignment is likely to depend on the properties of the gas disks and may reduce the angle between the spins and $\boldsymbol{L}$ to 10° (30°) for cold (hot) gas [63]. We emphasize here, that these angles are parameters valid at large separation and their validity as input parameters for kick formulae is still subject to the concerns raised in question 2. In the next section we will see that the inclusion of the long inspiral phase up to the last few orbits indeed has a profound statistical effect that may disfavor those spin-configuration leading to superkicks.

4 Spin-orbit resonances

A BH binary systems containing two spinning holes is characterized by 10 physical or *intrinsic* parameters: 2 BH masses m_1 and m_2, 6 parameters for the spins $\boldsymbol{S}_1$ and $\boldsymbol{S}_2$ and 2 parameters for the direction $\hat{\boldsymbol{L}}$ of the orbital angular momentum. The magnitude L is merely a measure of the separation of the BHs and does not characterize the actual system. The inspiral phase of a BH binary from large separations up to the last ~ 10 orbits is rather well modeled by PN theory [61] which in particular determines the time evolutions of the above parameters including the BH separation and thus L. The physical description is simplified significantly by eliminating 7 of these parameters as follows.

- BH binaries are invariant under a rescaling with the total mass $M = m_1 + m_2$ which leaves only one parameter for the mass ratio: $q = m_2/m_1$.
- At the PN orders considered, the BH masses and the individual BH spin magnitudes S_1, S_2 and the mass ratio q is conserved.
- We choose the z axis of our coordinate system such that it points in the direction of the orbital angular momentum.
- We choose the x axis such that it points in the direction of the projection of $\boldsymbol{S}_1$ into the orbital plane.

The time evolution of the system is therefore described by three remaining parameters which we choose to be the angles θ_1 and θ_2 between the individual BH spins and $\boldsymbol{L}$ and the angle $\Delta\Phi$ between the projections of $\boldsymbol{S}_1$ and $\boldsymbol{S}_2$ into the orbital plane; cf. Fig. 3. These angles can be directly obtained from the individual spins and the

orbital angular momentum whose time evolution is determined by the PN equations; see e.g. Appendix A in [59].

In general, the BH spins and $\boldsymbol{L}$ precess in a complicated way around the total angular momentum vector $\boldsymbol{J} \equiv \boldsymbol{L} + \boldsymbol{S}$, where $\boldsymbol{S} \equiv \boldsymbol{S}_1 + \boldsymbol{S}_2$. Schnittman [64], however, has found a subset of configurations where all three vectors $\boldsymbol{L}$, $\boldsymbol{S}_1$ and $\boldsymbol{S}_2$ are locked in a plane as they jointly precess around $\boldsymbol{J}$. These configurations are often referred to as "spin-orbit resonances" and are a consequence of the fact that the three time scales involved in a BH binary inspiral, the orbital time $t_{\rm orb}$, the precession time $t_{\rm pr}$ and the radiation reaction time scale $t_{\rm GW}$ obey a clear hierarchy $t_{\rm orb} \ll t_{\rm pr} \ll t_{\rm GW}$. Evidently, for these resonance configurations $\Delta\Phi = 0^\circ$ or $\Delta\Phi = \pm 180^\circ$ but Schnittman showed that for each of the two resonances there exist a one-parameter family of values (θ_1, θ_2) which remain constant on the precession time scale. On the much longer radiation reaction timescale, however, θ_1 and θ_2 slowly evolve while $\Delta\Phi$ remains constant at 0° or $\pm 180^\circ$. At a given moment in time we therefore have two curves in the θ_1-θ_2 plane, one curve for the $\Delta\Phi = 0^\circ$ resonance and one for the $\Delta\Phi = \pm 180^\circ$ resonance. As the BHs inspiral on the $t_{\rm GW}$ time scale, these two curves gradually sweep through the θ_1-θ_2 plane. Moreover, the resonances act as an attractor and capture freely precessing binaries into resonance or near-resonance configurations; cf. Figs. 6 and 7 in [64]. The resonances are illustrated in Fig. 4 for BH parameters $\boldsymbol{\chi}_1 = \boldsymbol{\chi}_2 = 1$ and $q = 9/11$. The resonant families are displayed as the solid (black) curves in the upper left ($\Delta\Phi = 0^\circ$) and the bottom right triangle ($\Delta\Phi = \pm 180^\circ$ resonance). The diagonal separating the two regions corresponds to $\theta_1 = \theta_2$. The figure demonstrates that $\theta_1 < \theta_2$ for the $\Delta\Phi = 0$ resonance solutions and $\theta_1 > \theta_2$ for the $\Delta\Phi = \pm 180^\circ$ resonance. This result is in fact general and applies to any choice of χ_1, χ_2 and q [64]. In the limit of infinite BH separation, the resonance curves coincide with the edges of the square. As the BHs inspiral, the resonance curves gradually approach the diagonal, but this motion is more pronounced for the $\Delta\Phi = 0^\circ$ family. For each family, the figure shows 6 curves corresponding to a BH separation $r = 1\,000\,M$, $500\,M$, $250\,M$, $100\,M$, $50\,M$ and $10\,M$. The dashed (red curves) represent the curves along which individual resonant binary systems evolve.

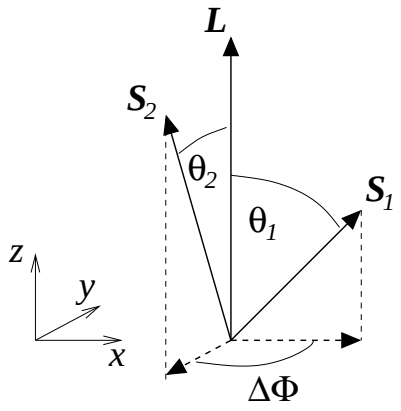

Fig. 3 The orbital angular momentum vector $\boldsymbol{L}$ and the individual BH spins $\boldsymbol{S}_1$, $\boldsymbol{S}_2$ define the angles θ_1, θ_2 and $\Delta\Phi$. x, y and z denote our specific choice of coordinates.

The short-dashed (blue) lines are curves of constant $\boldsymbol{S}\cdot\hat{\boldsymbol{L}}$ and the dash-dotted (green) lines are curves of constant $\boldsymbol{S}_0\cdot\hat{\boldsymbol{L}}$ where $\boldsymbol{S}_0\equiv(1+q)\boldsymbol{S}_1+(1+q^{-1})\boldsymbol{S}_2$. From the figure, and bearing in mind the attractive character of the resonance families, we can arrive at the following conclusions.

- Initially non-isotropic ensembles of spinning BH binaries can dramatically change their characteristics. In particular, binaries starting with $\theta_1<\theta_2$ (i.e. the more massive BH's spin is more aligned with $\boldsymbol{L}$) but with isotropic distribution in $\Delta\Phi$ are gradually captured by $\Delta\Phi=0^\circ$ resonances and therefore cluster near $\Delta\Phi=0^\circ$. Likewise, ensembles starting with $\theta_1>\theta_2$ (the more massive BH's spin is more misaligned with $\boldsymbol{L}$) preferentially cluster near $\Delta\Phi=\pm180^\circ$. This is important since superkick configurations have $\Delta\Phi=180^\circ$.
- As binary systems move towards the diagonal, θ_1 and θ_2 approach each other. For $\Delta\Phi=0^\circ$ resonances this means $\boldsymbol{S}_1$ and $\boldsymbol{S}_2$ align. For the $\Delta\Phi=\pm180^\circ$ resonances, instead, the angle θ_{12} between $\boldsymbol{S}_1$ and $\boldsymbol{S}_2$ approaches $\theta_1+\theta_2$.
- The dashed (red) and dash-dotted (green) lines in Fig. 4 are coincident (within numerical accuracy) in the figure. As the binaries inspiral the projection of the weighted spin $\boldsymbol{S}_0$ onto the orbital angular momentum is therefore conserved; an analytic calculation at the used PN order confirms this analysis [65]. The short-dashed (blue) curves corresponding to constant $\boldsymbol{S}\cdot\hat{\boldsymbol{L}}$ are steeper than the dashed (red) curves. The total spin $\boldsymbol{S}$ therefore becomes gradually more misaligned (aligned) with the orbital angular momentum for $\Delta\Phi=0^\circ$ ($\Delta\Phi=\pm180^\circ$) resonance configurations.

It can furthermore be shown that $\boldsymbol{S}_0\cdot\hat{\boldsymbol{L}}$ is also conserved for non-resonant binaries and the corresponding conclusions therefore apply for generic binaries. The most important conclusion for our discussion is the first item in the above list: binaries

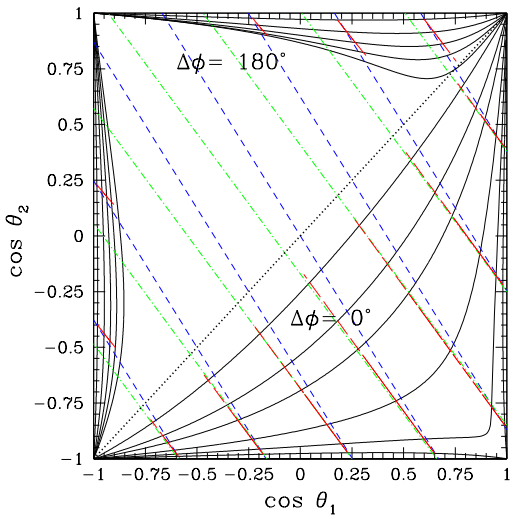

Fig. 4 Resonance families (black solid curves corresponding to $r=1000\,M$, $500\,M$, $250\,M$, $100\,M$, $50\,M$ and $10\,M$ from the square's edges inwards) are shown in the θ_1-θ_2 plane. As resonant binaries inspiral, they move towards the diagonal $\theta_1=\theta_2$ along the red dashed lines with $\boldsymbol{S}_0\cdot\hat{\boldsymbol{L}}=$ const. It can be shown that freely precessing binaries move along the same lines, although not in monotonic fashion towards the diagonal but back and forth. The blue short-dashed curves correspond to constant $\boldsymbol{S}\cdot\hat{\boldsymbol{L}}$ and green dash-dotted curves to constant $\boldsymbol{S}_0\cdot\hat{\boldsymbol{L}}$. Figure taken from [65].

are attracted towards $\Delta\Phi = 0^\circ$ ($\Delta\Phi = \pm 180^\circ$)) if the more massive (the less massive) BH's spin is more aligned with the orbital angular momentum. The intuitive conclusion is that preferential alignment (misalignment) of the more massive BH with $\boldsymbol{L}$ leads to a statistical suppression (enhancement) of superkicks. We shall see that this is indeed the case in the next section.

5 Suppression of superkicks

The impact of the spin-orbit resonances on the recoil velocities is of statistical nature. We have seen that for a given ensemble of BH binaries, the distribution of the BH spins, characterized by the angles θ_1, θ_2 and $\Delta\Phi$, can change substantially as the binaries inspiral from $r = 1\,000\,M$ to $r = 10\,M$. In order to quantify the resulting effect on the expected kick distribution, we consider two types of ensembles with fixed values $\chi_1 = \chi_2 = 1$, $q = 9/11$. Ensemble 1 contains $10 \times 10 \times 10$ binaries equally spaced in $\Delta\Phi = [-180^\circ, 180^\circ)$ and $\cos\theta_1, \cos\theta_2 \in [0,1]$, i.e. with isotropic distribution in the spin directions. Ensembles of type 2 consist of 30×30 binaries equally spaced in $\cos\theta_2$ and $\Delta\Phi$ but with a fixed value of θ_1. We consider six ensembles of type 2 for the specific values $\theta_1 = 10^\circ$, 20°, 30°, 150°, 160° and 170°. Ensembles with a small θ_1 represent binaries where the more massive BH is preferentially more aligned with $\boldsymbol{L}$ whereas those ensembles with large θ_1 have the less massive BH preferentially aligned with $\boldsymbol{L}$. From the results of the previous section, we expect the former to be attracted by the $\Delta\Phi = 0^\circ$ resonances and therefore to result in smaller kicks. For large θ_1 we expect the converse.

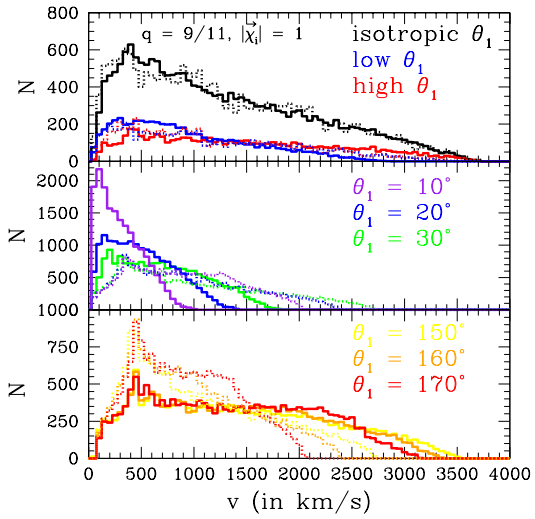

Fig. 5 Histograms of the kick distribution obtained for Ensemble 1 (top panel) and six ensembles of type 2 (center and bottom panel). Dashed curves are obtained for the BH binary parameters as initialized at large separation $r = 1\,000\,M$ and solid curves are obtained for the parameters at the end of the inspiral $r = 10\,M$. Changes in the histograms due to the inspiral depend on whether the more massive BH is initially more aligned (small values of θ_1) or more misaligned (large values of θ_1) with the orbital angular momentum $\boldsymbol{L}$. Figure taken from [51].

This expectation is borne out in Fig. 5 which displays histograms of the recoil velocities for the different ensembles. Let us first consider the upper panel of the figure. The dashed black curve shows the kick distribution for Ensemble 1 as predicted by Eq. (3) for the input parameters of the binaries at the start of the inspiral, i.e. at $r = 1\,000\,M$. Likewise, the solid black curve shows the distribution when using the BH binary parameters at the end of the inspiral, i.e. at $r = 10\,M$. Ensemble 1 is an isotropic ensemble and as we have already discussed in the previous section, initially isotropic ensembles remain isotropic under the inspiral and the corresponding kick distributions are identical up to statistical noise. The blue (red) curves in the same panel correspond to subsets of Ensemble 1 containing only those 30 % of the entire ensemble with the lowest (highest) values of θ_1. For these non-isotropic subsets we observe the expected change in the kick distribution. For ensembles where the more massive BH is more (less) aligned with the orbital angular momentum, that is for the "blue" ("red") ensembles, the kick distribution obtained for the parameters at the end of the inspiral is shifted towards smaller (larger) kick velocities. This is displayed in more detail in the center and bottom panel of the figure where the six ensembles of type 2 are displayed, again in the form of dashed curves for the initial values of θ_1, θ_2 and $\Delta\Phi$ at $r = 1\,000\,M$ and solid curves for the values at the end of the inspiral at $r = 10\,M$. The central panels contains ensembles with $\theta_1 = 10^\circ$ (purple), $\theta_1 = 20^\circ$ (blue) and $\theta_1 = 30^\circ$ (green). The kick distribution after inspiral is notably shifted towards smaller $v_{\rm kick}$, the effect being stronger the smaller θ_1. The opposite is observed in the bottom panel where $\theta_1 = 150^\circ$ (yellow), $\theta_1 = 160^\circ$ (orange) and $\theta_1 = 170^\circ$ (red curves). The larger θ_1 is fixed initially, the more strongly the distributions are shifted towards larger $v_{\rm kick}$ after the inspiral.

We have focused here on maximal spin magnitude $\chi_1 = \chi_2 = 1$ and mass ratio $q = 9/11$. The complete study performed by Kesden *at al.* [51, 51] also considers smaller spin magnitudes 0.75, 0.5 and 0.25 as well as other mass ratios $q = 2/3$ and $1/3$. The kick suppression or enhancement due to the spin-orbit resonances becomes less pronounced for smaller values of the spin magnitude and mass ratio. In these cases, however, the kick velocities are significantly smaller anyway (whether including resonance effects or not), so that alterations to the distribution due to capture by resonances during the inspiral are less important in the context of BH ejections or displacement from the centers of galaxies. See Figs. 3, 4 and Table 1 in [51] for more quantitative details.

We finally note that the kick formula used for this investigation is given by Eq. (3) and therefore does not include that hang-up effect in the recoil velocities. A similar study to that described above has been done for the hang-up kicks in Ref. [66], however, and observed the same suppression (enhancement) of kick distributions when using more recent formula by Lousto & Zlochower [47, 48]. The effective suppression or enhancement of hang-up kicks due to resonant capture may appear surprising at first glance since partial alignment of the individual BH spins with $\boldsymbol{L}$ is a vital ingredient in the hang-up kicks. The key angle affected by the resonances, however, is $\Delta\Phi$. And BH configurations leading to superkicks or hang-up kicks always require $\Delta\Phi \approx 180^\circ$. As we have seen, the resonances tend to push BH binaries either close to this value of $\Delta\Phi$ (when the more massive BH is preferentially mis-

aligned with $\boldsymbol{L}$, i.e. large θ_1) or to the opposite extreme $\Delta\Phi = 0^\circ$ (when the more massive BH is preferentially aligned with $\boldsymbol{L}$, i.e. small θ_1).

Given these results, there remains one important outstanding question: is the more massive BH preferentially aligned with the orbital angular momentum or not? The answer to this question ultimately has to come from astrophysics and, in particular, detailed studies of the interaction of the individual BHs in a binary with surrounding accretion disks from the point of formation of the binary system up to the point where the inspiral is driven by GW emission, i.e. up to separations $r \sim 1\,000\,M$. The seemingly ubiquitous presence of SMBHs at the center of galaxies may indicate that superkicks are indeed suppressed and therefore suggest stronger alignment of the more massive BH but the answer to this question remains at present unknown.

6 Conclusions

Gravitational recoil generated by the emission of anisotropic gravitational radiation may manifest itself in a variety of observational features of galaxies and is likely to play an important role in the formation of galaxies and the assembly of the observed SMBHs. The observational signatures in the electromagnetic spectrum include double active galactic nuclei, X ray flares and Doppler shifts between the broad and narrow-line regions of quasars.

Following the breakthroughs in numerical relativity, it has been possible to obtain precision estimates for the magnitude of the kick velocities as functions of the BH parameters. The most astounding result of these studies has been the discovery of the *superkicks* of several thousand km/s generated for BH binaries with comparable mass and spin components in the orbital plane that are equal in magnitude and opposite in direction. These kicks are comfortably large enough to eject BHs from even the most massive host galaxies and may explain some of the observed features mentioned above although kicks are not the only explanations for these observations.

The large magnitude of the superkicks naturally prompts the question why SMBHs do not appear to be efficiently kicked out of their host galaxies. The answer to this question may simply be of statistical nature and BH ejection may feature more prominently in larger future surveys. There are indications, however, that superkick configurations may not be the favored arrangements in astrophysical binaries. Accretion torques tend to align the BH spins with the orbital angular momentum. During the GW driven inspiral all the way to merger, spin-orbit resonances are likely to populate preferentially specific portions of the parameter space. This effect depends on whether the more massive BH is initially more or less aligned with the orbital angular momentum. In the former case, kicks are suppressed whereas in the latter case kicks can even be enhanced. It is at present unknown which of these scenarios is more common. Future observations of the BH occupation fraction of galaxies should provide valuable insight into this question. Either way, the spin-

orbit resonances demonstrate the importance of including the long GW driven inspiral in the usage of BH parameters in formulae predicting kick velocities. Further calibration of these kick formulae is also required, in particular to obtain accurate determination of the hang-up or superkicks' dependency on the mass ratio.

Acknowledgements The author thanks E. Berti, D. Gerosa, K. Kesden, R. O'Shaughnessy for many fruitful discussions. This work was supported by NSF-XSEDE Grant No. PHY-090003, FP7-PEOPLE-2011-CIG Grant No. 293412 "CBHEO", FP7-PEOPLE-2011-IRSES Grant No.295189 "NRHEP", STFC GR Roller Grant No. ST/L000636/1, the Cosmos system, part of DiRAC, funded by STFC and BIS under Grant Nos. ST/K00333X/1 and ST/J005673/1, ERC-2010-StG Grant No. DyBHo, and CESGA Grant No. ICTS-2013-249. Computations were performed on the Cambridge Cosmos system, the SDSC Trestles and NICS Kraken clusters, and CESGA's Finis Terra.

References

1. Google Dictionary: `http://google-dictionary.so8848.com/`
2. A. Wongwathanarat, H.T. Janka, E. Mueller, A&A 552, **A126** (2013). DOI 10.1051/0004-6361/201220636. ArXiv:1210.8148 [astro-ph]
3. W.B. Bonnor, M.A. Rotenberg, Proc. R. Soc. Lond. A. **265**, 109 (1961)
4. A. Peres, Phys. Rev. **128**, 2471 (1962)
5. J.D. Bekenstein, Astrophys. J. **183**, 657 (1973). DOI 10.1086/152255
6. D. Merritt, M. Milosavljević, M. Favata, S. Hughes, D. Holz, Astrophys. J. **607**, L9 (2004). DOI 10.1086/421551. Astro-ph/0402057
7. J. Kormendy, D. Richstone, Ann. Rev. Astron. Astrophys. **33**, 581 (1995). DOI 10.1146/annurev.aa.33.090195.003053
8. J. Magorrian, S. Tremaine, D. Richstone, R. Bender, G. Bower, A. Dressler, S.M. Faber, K. Gebhardt, R. Green, C. Grillmair, J. Kormendy, T. Lauer, Astron. J **115**, 2285 (1998). DOI 10.1086/300353. Astro-ph/9708072
9. L. Ferrares, D. Merritt, Astrophys. J **539**, L9 (2000). DOI 10.1086/312838. Astro-ph/0006053
10. K. Gebhardt, R. Bender, G. Bower, A. Dressler, S.M. Faber, A.V. Filippenko, R. Green, C. Grillmair, L.C. Ho, J. Kormendy, T.R. Lauer, J. Magorrian, J. Pinkney, S. Richstone, D. Tremaine, Astrophys. J **539**, L13 (2000). DOI 10.1086/312840. Astro-ph/0006289
11. M. Volonteri, F. Haardt, P. Madau, Astrophys. J **582**, 559 (2003). DOI 10.1086/344675. Astro-ph/0207276
12. M. Micic, T. Abel, S. Sigurdsson, MNRAS **372**, 1540 (2006). DOI 10.1111/j.1365-2966.2006.11013.x. Astro-ph/0512123
13. K. Holley-Bockelmann, K. Gultekin, D. Shoemaker, N. Yunes, Astrophys. J. **686**, 829 (2008). DOI 10.1086/591218. ArXiv:0707.1334 [astro-ph]
14. M.C. Miller, V.M. Lauburg, Astrophys. J. **692**, 917 (2009). DOI 10.1088/0004-637X/692/1/917. ArXiv:0804.2783 [astro-ph]
15. I. Mandel, D.A. Brown, J.R. Gair, M.C. Miller, Astrophys.J. **681**, 1431 (2008). DOI 10.1086/588246. ArXiv:0705.0285 [astro-ph]
16. Z. Haiman, Astrophys. J **613**, 36 (2004). DOI 10.1086/422910. Astro-ph/0404196
17. S. Komossa, H. Zhou, H. Lu, Astrophys. J. **678**, L81 (2008). DOI 10.1086/588656. ArXiv:0804.4585 [astro-ph]
18. T. Bogdanović, M. Eracleous, S. Sigurdsson, Astrophys.J. **697**, 288 (2009). DOI 10.1088/0004-637X/697/1/288. ArXiv:0809.3262 [astro-ph]
19. G. Shields, E. Bonning, S. Salviander, Astrophys. J. **696**, 1367 (2009). DOI 10.1088/0004-637X/696/2/1367. ArXiv:0810.2563 [astro-ph]
20. L. Blecha, F. Civano, M. Elvis, A. Loeb, (2012). ArXiv:1205.6202 [astro-ph]

21. J. Wrobel, J. Comerford, E. Middelberg, Astrophys.J. **782**, 116 (2014). DOI 10.1088/0004-637X/782/2/116. ArXiv:1401.4756 [astro-ph]
22. S. Komossa, N. Bade, Astron. Astroph. **343**, 775 (1999). Astro-ph/9901141
23. S. Komossa, D. Merritt, Astrophys. J. **683**, L21 (2008). DOI 10.1086/591420. ArXiv:0807.0223 [astro-ph]
24. J.S. Bloom, et al., Science **333**, 203 (2011). DOI 10.1126/science.1207150. ArXiv:1104.3257 [astro-ph]
25. S. Komossa, D. Merritt, Astrophys. J. **689**, L89 (2008). DOI 10.1086/595883. ArXiv:0811.1037 [astro-ph]
26. F.D. Lora-Clavijo, F.S. Guzmán, MNRAS **429**, 3144 (2013). DOI 10.1093/mnras/sts573. ArXiv:1212.2139 [astro-ph]
27. S. Komossa, Adv. Astron. **2012**, 364973 (2012). DOI 10.1155/2012/364973. ArXiv:1202.1977 [astro-ph]
28. M.J. Fitchett, MNRAS **203**, 1049 (1983)
29. P.C. Peters, Phys. Rev. **136**, B1224 (1964). DOI 10.1103/PhysRev.136.B1224
30. F. Pretorius, Phys. Rev. Lett. **95**, 121101 (2005). DOI 10.1103/PhysRevLett.95.121101. Gr-qc/0507014
31. J.G. Baker, J. Centrella, D.I. Choi, M. Koppitz, J. van Meter, Phys. Rev. Lett. **96**, 111102 (2006). DOI 10.1103/PhysRevLett.96.111102. Gr-qc/0511103
32. M. Campanelli, C.O. Lousto, P. Marronetti, Y. Zlochower, Phys. Rev. Lett. **96**, 111101 (2006). DOI 10.1103/PhysRevLett.96.111101. Gr-qc/0511048
33. J.A. Gonzalez, U. Sperhake, B. Brügmann, Phys. Rev. D **79**, 124006 (2009). DOI 10.1103/PhysRevD.79.124006. ArXiv:0811.3952 [gr-qc]
34. J.G. Baker, J. Centrella, D.I. Choi, M. Koppitz, J. van Meter, M.C. Miller, Astrophys. J **653**, L93 (2006). DOI 10.1086/510448. Gr-qc/0603204
35. J.A. González, U. Sperhake, B. Brügmann, M.D. Hannam, S. Husa, Phys. Rev. Lett. **98**, 091101 (2007). DOI 10.1103/PhysRevLett.98.091101. Gr-qc/0610154
36. F. Herrmann, I. Hinder, D. Shoemaker, P. Laguna, Class. Quantum Grav. **24**, S33 (2007). DOI 10.1088/0264-9381/24/12/S04. Gr-qc/0601026
37. J.D. Schnittman, A. Buonanno, Astrophys. J. **662**, L63 (2007). DOI 10.1086/519309. Astro-ph/0702641
38. L.E. Kidder, Phys. Rev. D **52**, 821 (1995). DOI 10.1103/PhysRevD.52.821. Gr-qc/9506022
39. F. Herrmann, I. Hinder, D. Shoemaker, P. Laguna, R.A. Matzner, Astrophys. J. **661**, 430 (2007). DOI 10.1086/513603. Gr-qc/0701143
40. M. Koppitz, D. Pollney, C. Reisswig, L. Rezzolla, J. Thornburg, P. Diener, E. Schnetter, Phys. Rev. Lett. **99**, 041102 (2007). DOI 10.1103/PhysRevLett.99.041102. Gr-qc/0701163
41. D. Pollney *et al.*, Phys. Rev. D **76**, 124002 (2007). DOI 10.1103/PhysRevD.76.124002. ArXiv:0707.2559 [gr-qc]
42. J.A. González, M.D. Hannam, U. Sperhake, B. Brügmann, S. Husa, Phys. Rev. Lett. **98**, 231101 (2007). DOI 10.1103/PhysRevLett.98.231101. Gr-qc/0702052
43. M. Campanelli, C.O. Lousto, Y. Zlochower, D. Merritt, Astrophys. J. **659**, L5 (2007). DOI 10.1086/516712. Gr-qc/0701164
44. M. Campanelli, C.O. Lousto, Y. Zlochower, D. Merritt, Phys. Rev. Lett. **98**, 231102 (2007). DOI 10.1103/PhysRevLett.98.231102. Gr-qc/0702133
45. B. Brügmann, J.A. González, M.D. Hannam, S. Husa, U. Sperhake, Phys. Rev. D **77**, 124047 (2008). DOI 10.1103/PhysRevD.77.124047. ArXiv:0707.0135 [gr-qc]
46. F. Pretorius, in *Physics of Relativistic Objects in Compact Binaries: From Birth to Coalescence*, ed. by M. Colpi *et al.* (Springer, New York, 2009). ArXiv:0710.1338 [gr-qc]
47. C.O. Lousto, Y. Zlochower, Phys. Rev. Lett. **107**, 231102 (2011). DOI 10.1103/PhysRevLett.107.231102. ArXiv:1108.2009 [gr-qc]
48. C.O. Lousto, Y. Zlochower, M. Dotti, M. Volonteri, Phys. Rev. D **85**, 084015 (2012). DOI 10.1103/PhysRevD.85.084015. ArXiv:1201.1923 [gr-qc]
49. M. Campanelli, C.O. Lousto, Y. Zlochower, Phys. Rev. D **74**, 041501 (2006). DOI 10.1103/PhysRevD.74.041501. Gr-qc/0604012

50. G. Lovelace, M. Boyle, M.A. Scheel, B. Szilágyi, Class. Quantum Grav. **29**, 045003 (2012). DOI 10.1088/0264-9381/29/4/045003. ArXiv:1110.2229 [gr-qc]
51. M. Kesden, U. Sperhake, E. Berti, Astrophys. J. **715**, 1006 (2010). DOI 10.1088/0004-637X/715/2/1006. ArXiv:1003.4993 [astro-ph]
52. C.O. Lousto, Y. Zlochower, Phys. Rev. D **79**, 064018 (2009). DOI 10.1103/PhysRevD.79.064018. ArXiv:0805.0159 [gr-qc]
53. C.O. Lousto, Y. Zlochower, Phys. Rev. D **77**, 044028 (2008). DOI 10.1103/PhysRevD.77.044028. ArXiv:0708.4048 [gr-qc]
54. L. Boyle, M. Kesden, S. Nissanke, Phys. Rev. Lett. **100**, 151101 (2008). DOI 10.1103/PhysRevLett.100.151101. ArXiv:0709.0299 [gr-qc]
55. L. Boyle, M. Kesden, Phys. Rev. D **78**, 024017 (2008). DOI 10.1103/PhysRevD.78.024017. ArXiv:0712.2819 [astro-ph]
56. C.O. Lousto, Y. Zlochower, Phys. Rev. D **87**(8), 084027 (2013). DOI 10.1103/PhysRevD.87.084027. ArXiv:1211.7099 [gr-qc]
57. J.G. Baker, et al., Astrophys. J. **668**, 1140 (2008). DOI 10.1086/521330. Astro-ph/0702390
58. J.G. Baker *et al.*, Astrophys.J. **682**, L29 (2008). DOI 10.1086/590927. ArXiv:0802.0416 [astro-ph]
59. D. Gerosa, M. Kesden, E. Berti, R. O'Shaughnessy, U. Sperhake, Phys. Rev. D **87**, 104028 (2013). DOI 10.1103/PhysRevD.87.104028. ArXiv:1302.4442 [gr-qc]
60. T. Bogdanović, C.S. Reynolds, M.C. Miller, Astrophys. J. **661**, L147 (2007). DOI 10.1086/518769. Astro-ph/0703054
61. L. Blanchet, Living Reviews in Relativity **9**(4) (2006). http://www.livingreviews.org/lrr-2006-4
62. D. Gerosa, A. Sesana, (2014). ArXiv:1405.2072 [astro-ph]
63. M. Dotti, M. Volonteri, A. Perego, M. Colpi, M. Ruszkowski, F. Haardt, MNRAS **402**, 682 (2009). ArXiv:0910.5729 [astro-ph]
64. J.D. Schnittman, Phys. Rev. D **70**, 124020 (2004). DOI 10.1103/PhysRevD.70.124020. Astro-ph/0409174
65. M. Kesden, U. Sperhake, E. Berti, Phys. Rev. D **81**, 084054 (2010). DOI 10.1103/PhysRevD.81.084054. ArXiv:1002.2643 [astro-ph]
66. E. Berti, M. Kesden, U. Sperhake, Phys. Rev. D **85**, 124049 (2012). DOI 10.1103/PhysRevD.85.124049. ArXiv:1203.2920 [astro-ph]